

Femtosecond pulse shaping by dynamic holograms in photorefractive multiple quantum wells

Y. Ding, R. M. Brubaker, and D. D. Nolte

Department of Physics, 1396 Physics Building, Purdue University, West Lafayette, Indiana 47907-1396

M. R. Melloch and A. M. Weiner

School of Electrical Engineering, Purdue University, West Lafayette, Indiana 47907

Received December 9, 1996

Femtosecond pulses can be shaped in the time domain by diffraction from dynamic holograms in a photorefractive multiple quantum well placed inside a Fourier pulse shaper. We present several examples of shaped pulses obtained by controlling the amplitude or the phase of the hologram writing beams, which modifies the complex spectrum of the femtosecond output. © 1997 Optical Society of America

In applications in optical communication and information processing, the ability arbitrarily to manipulate ultrafast pulses is of great interest and practical importance. The use of femtosecond lasers offers possibilities of exploiting the large bandwidth of optics. Shaping laser pulses on the femtosecond (fs) time scale was demonstrated in 1988.¹ Since then, extensive research has been done in this area,²⁻⁸ much of it based on Fourier synthesis techniques in which the optical frequency components of a fs pulse are manipulated by an amplitude or phase mask in the Fourier domain. By changing the mask, one can obtain different-shaped pulses. Such an apparatus is usually called a pulse shaper. Either permanent transmission or holographic masks made by microlithography techniques or programmable spatial light modulators can be put into the pulse shaper.²⁻⁷ Picosecond pulse shaping experiments using bulk photorefractive materials⁸ have demonstrated the possibility of real-time control over the hologram, limited only by the material response time. Photorefractive multiple quantum wells (MQW's) have high nonlinear sensitivities ($\Delta n \sim 10^{-2}$) with small driving intensities ($\sim 10 \mu\text{W}/\text{cm}^2$) and fast response times ($\sim \mu\text{s}$).⁹⁻¹¹ The holograms in MQW's are thin, and the diffraction is in the Raman-Nath regime. No Bragg matching is necessary, which makes the alignment of the system simpler. MQW's can also be designed by band-gap engineering to match different application wavelengths, such as $1.55 \mu\text{m}$ for optical fiber communications.¹² In the femtosecond regime, photorefractive MQW's were previously used for electric-field cross-correlation measurements¹¹ and for time-to-space conversion experiments.¹³ We report here, for the first time to our knowledge, the experimental demonstration of femtosecond pulse shaping with photorefractive MQW's in a pulse shaper.

Figure 1 shows the top view of the experimental setup, which eliminates temporal dispersion and permits a possible synthesis of fs pulses. The setup is similar to that of the standard pulse shaper,¹ with two differences related to the use of dynamic holography. First, a photorefractive MQW instead of a mask

is placed in the Fourier plane in the pulse shaper. The hologram is written in the MQW by two beams from a cw diode laser operating at 685 nm. The power of each writing beam is 2 mW. Second, the lenses used in the pulse shaper are cylindrical instead of the conventional spherical lenses. When cylindrical lenses are used, the incident fs beam is not focused in the vertical direction, ensuring an appropriate intensity ratio between the unfocused cw writing beams and the fs probe beam to prevent the photorefractive grating from being erased, leading to the optimal diffraction signal. The Fourier transform of the fs probe beam in the horizontal direction remains. A laser beam with a pulse width of 120 fs, a central wavelength of 847 nm, and a repetition rate of 100 MHz is incident upon the first grating of the pulse shaper, where it is dispersed in the horizontal plane. The separated frequency components are diffracted from the photorefractive grating in the vertical plane determined by the two writing beams. The

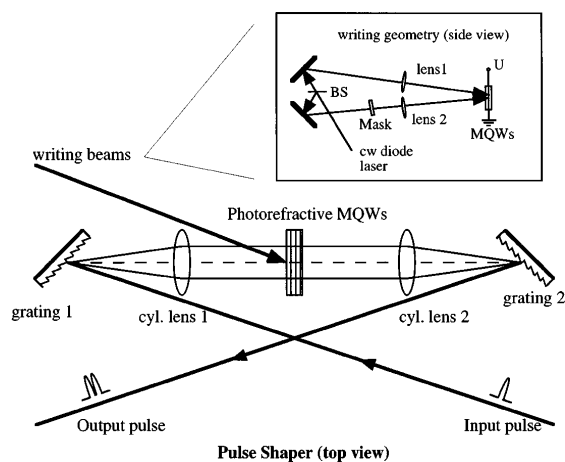


Fig. 1. Experimental setup for femtosecond pulse shaping using photorefractive gratings written in MQW's. The focusing length of the cylindrical lenses in the pulse shaper is 10 cm, and the two gratings have a groove density of 1800 lines/mm, leading to a spatial spectrum separation of 0.36 mm/nm. The inset shows the writing geometry on the vertical plane. BS, beam splitter; U, applied voltage.

diffracted optical components are Fourier transformed by the second cylindrical lens and recombined by the second grating, forming the fs output pulse carrying the information of the photorefractive grating. The use of vertical writing geometry solves the problem of the phase difference between the diffracted frequency components that is due to the diffraction angle.⁸ The shape of the pulse is measured by electric-field cross correlation with an unshaped reference pulse, which is an approximately transform-limited Gaussian pulse. Electric-field cross correlation is a technique by which one measures the interference between the signal pulse and a reference pulse with a known shape by scanning the time delay between the two pulses. An imaging lens ($f = 200$ mm) is put into one of the writing beams to project a mask onto the MQW (with an amplification of 2.2 in our experiments). An identical lens is used in the second writing beam to compensate for the wavefront difference between the two writing beams that is due to the imaging lens, which would extend the fs pulse into the picosecond time scale. The pulse shaper is carefully aligned to be dispersion free with no MQW in it, yielding output pulses identical to the incident ones. A photorefractive GaAs/Al_{0.1}Ga_{0.9}As MQW is then placed in the Fourier plane. A dc electric field of 3 kV/cm is applied on the MQW (with transverse field geometry). The photorefractive grating spacing is approximately 11 μm , and the output diffraction efficiency is of the order of 10^{-3} . The diffracted pulse from the pulse shaper without any mask is broadened by approximately a factor of 2, determined by the bandwidth of the excitonic absorption of the MQW.

In MQW's both electroabsorption and electrorefraction vary strongly with frequency. One might expect strong phase changes in the diffracted pulse. For pulse shaping applications, however, it is important to have a flat or linear phase of the diffracted pulse for each frequency component. A linear phase with frequency yields only a delay, not a distortion, in the pulse shape. We verify that our MQW has such a feature within the MQW bandwidth by using spectral interferometry¹⁴ to measure the phase of the diffracted pulse without any masks, where the spectrum of a reference pulse interferes with that of the diffracted pulse, which is delayed by 1500 fs. Figure 2 shows the spectral interferometry pattern and the phase of the diffracted pulse extracted from it with a linear part subtracted. The phase is quite flat (linear) around the center wavelength of 847 nm.

The linear phase is a result of the character of the transverse-field MQW devices, where electroabsorption is due to the broadening of the transition line shape. The characteristic electroabsorption spectrum $\Delta\alpha(\omega)$ is approximately a second derivative of a Gaussian transition line shape,⁹ which is an even function. (Near the absorption center, it can be described in form of a cosine function plus some vanishing higher-order harmonics.) The electrorefraction $\Delta n(\omega)$ is related to $\Delta\alpha(\omega)$ by the Kramers-Kronig relation, which transforms an even function into an odd one (a cosine function is transformed into a -sine function). Because the first-order diffraction is proportional to the photorefractive grating, $i\Delta\tilde{n}(\omega) = i[\Delta n(\omega) + i\Delta\alpha(\omega)/2k]$,

it has an even real part and an odd imaginary part. In the frequency domain the phase is given by $\varphi = \arctan(2k\Delta n/\Delta\alpha)$ and is approximately a linear function with frequency. In the time domain the diffracted pulse is the Fourier transform of the diffracted field in the frequency domain, resulting in a purely real function even without this linear approximation.

To shape the pulse, one places a mask into one of the writing beams, as shown in Fig. 1, to modify the MQW photorefractive grating in the pulse shaper. By changing the position of the mask and the imaging lenses, one can project either the image (as in the current experiments) or the Fourier transform of the mask onto the MQW in the pulse shaper. Therefore the resulting temporal pulses are related either to the Fourier transform of the mask (as here) or potentially to the mask directly. This feature permits more flexible pulse processing than in an ordinary pulse shaper.

As a first example, we placed a fixed phase mask into one of the writing beams, imaging it into the MQW sample. The mask contained a single $0/0.9\pi$ phase step, which changed the phase of one half of the writing beam by 0.9π with respect to the other half. The diffracted beam from the grating with the phase step then experienced a phase function

$$H(\omega) = \begin{cases} 1 & -\infty < \omega \leq \omega_c \\ \exp(i0.9\pi) & \omega_c \leq \omega < \infty \end{cases}, \quad (1)$$

with the center frequency ω_c . The output electric field in the frequency domain became

$$E_{\text{out}}(\omega) = E_{\text{in}}(\omega)H(\omega)f(\omega), \quad (2)$$

where $E_{\text{in}}(\omega)$ is the Gaussian incident field and $f(\omega)$ is a function describing the diffraction from the photorefractive grating in the MQW materials. The output pulse in the time domain is the Fourier transform of $E_{\text{out}}(\omega)$, which resulted in a double pulse. The experimental data of the electric-field cross correlation and the envelope extracted from the data are shown in Fig. 3(a).

In Fig. 3(b) we show a second example, in which a double-slit amplitude mask was imaged onto the MQW. The slit width was ~ 250 μm , with a separation of 330 μm . The double slit pattern at the Fourier

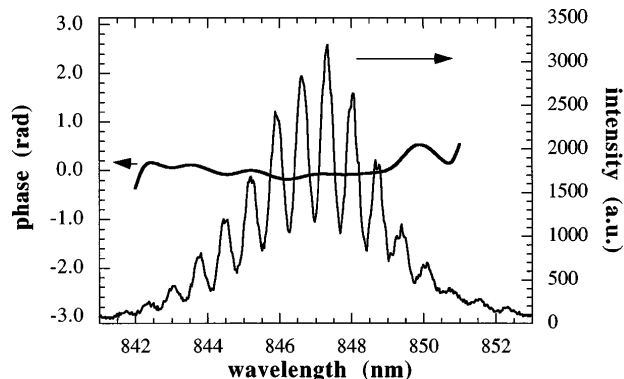


Fig. 2. Phase of the beam diffracted from the MQW in the pulse shaper, extracted from the spectral interference between the reference pulse and the diffracted pulse.

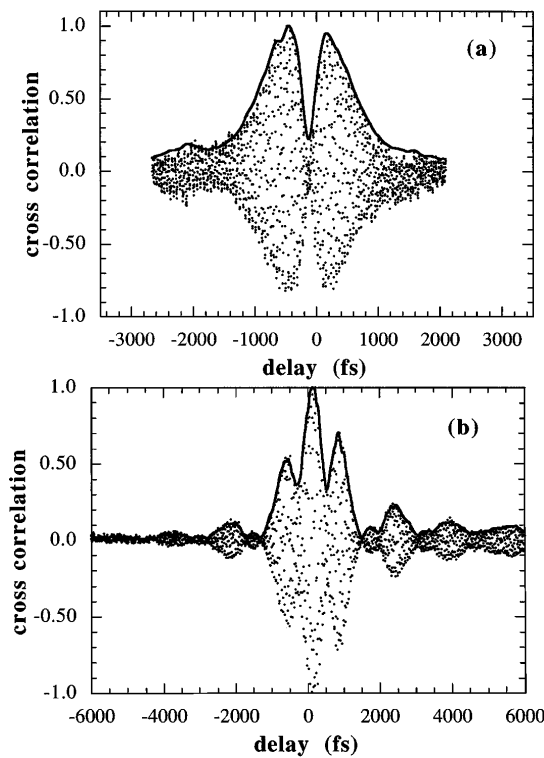


Fig. 3. Electric-field cross-correlation data and the extracted envelope of a shaped fs pulse when (a) a $0/0.9\pi$ phase step mask and (b) a double-slit amplitude mask was introduced into the writing beam.

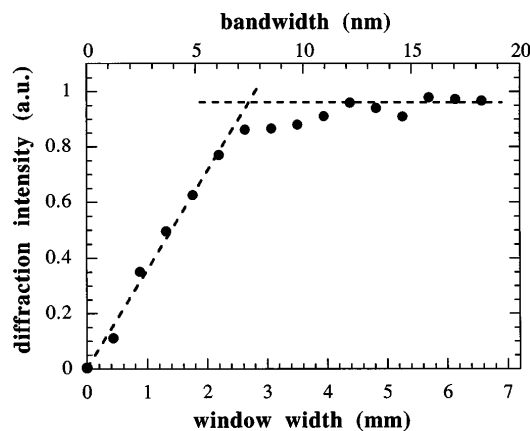


Fig. 4. Diffraction intensity as a function of the window width at the Fourier plane controlled by a single slit, showing the bandwidth limitation of the MQW sample. The dashed lines are guides for the eye.

plane allowed only two discrete frequency groups to be diffracted, resulting in a double-slit interference pattern in the time domain. In this case, $H(\omega)$ in Eq. (2) is

$$H(\omega) = B(\omega - \omega_s/2) + B(\omega + \omega_s/2), \quad (3)$$

with the frequency separation ω_s (the corresponding wavelength separation is 2 nm in our experiment) and the box function of width ω_w :

$$B(\omega) = \begin{cases} 1 & |\omega| \leq \omega_w/2 \\ 0 & |\omega| > \omega_w/2 \end{cases}. \quad (4)$$

The Fourier transform of $E_{\text{out}}(\omega)$ in Eq. (2) gives a typical double-slit interference pattern, as we experimentally observed.

The pulse manipulation can also be used to check the bandwidth limitation of the photorefractive MQW's. The power spectrum of the diffracted beam without any mask is nearly Gaussian, with a FWHM of 3.9 nm, whereas that of the input beam is 8 nm. To check the bandwidth limitation of the MQW, we measured the diffracted beam intensity as a function of the width of the spectral window (Fig. 4). The spectral window was controlled by the spatial width of the photorefractive grating by use of a varying single slit in the writing beam, which as before was imaged onto the MQW. The diffraction signal began to drop at a grating width of 3.5 mm and reached its half value at a width of 1.4 mm, corresponding to a spectral window width of 3.89 nm, which agrees well with the spectrum measurement.

In conclusion, we have demonstrated the application of photorefractive MQW's as dynamic diffractive masks for femtosecond pulse shaping. This technique makes femtosecond pulse shaping more flexible by performing the frequency filtering outside the pulse shaper.

The authors gratefully acknowledge support from the U.S. Department of Defense Focused Research Initiative through U.S. Air Force Office of Scientific Research grant F49620-95-1-0533, National Science Foundation grant 9414800-ECS, and Rome Labs grant F30602-96-2-0114. R. M. Brubaker acknowledges support from Eastman Kodak Company as a Kodak Fellow.

References

1. A. M. Weiner, J. P. Heritage, and E. M. Kirschner, *J. Opt. Soc. Am. B* **5**, 1563 (1988).
2. A. M. Weiner, D. E. Leaird, J. S. Patel, and J. R. Wullert, *Opt. Lett.* **15**, 326 (1990).
3. A. M. Weiner, D. E. Leaird, J. S. Patel, and J. R. Wullert, *IEEE J. Quantum Electron.* **28**, 908 (1992).
4. A. M. Weiner, *Prog. Quantum Electron.* **19**, 161 (1995).
5. M. M. Wefers, K. A. Neilson, and A. M. Weiner, *Opt. Lett.* **21**, 746 (1996).
6. K. Ema and F. Shimizu, *Jpn. J. Appl. Phys.* **29**, L631 (1990).
7. M. C. Nuss and R. L. Morisson, *Opt. Lett.* **20**, 740 (1995).
8. K. Ema, *Jpn. J. Appl. Phys.* **30**, L2046 (1991).
9. D. D. Nolte and M. R. Melloch, in *Photorefractive Effects and Materials*, D. Nolte, ed. (Kluwer, Dordrecht, The Netherlands, 1995).
10. Q. N. Wang, R. M. Brubaker, D. D. Nolte, and M. R. Melloch, *J. Opt. Soc. Am. B* **9**, 1626 (1992).
11. R. M. Brubaker, Q. N. Wang, D. D. Nolte, E. S. Harmon, and M. R. Melloch, *J. Opt. Soc. Am. B* **11**, 1038 (1994).
12. C. De Matos, A. Le Corre, H. L'Haridon, B. Lambert, S. Salaün, J. Pleumeeckers, and S. Gosselin, *Appl. Phys. Lett.* **68**, 517 (1996).
13. M. C. Nuss, M. Li, T. H. Chiu, A. M. Weiner, and A. Partovi, *Opt. Lett.* **19**, 664 (1994).
14. L. Lepetit, G. Cheriaux, and M. Joffre, *J. Opt. Soc. Am. B* **12**, 2467 (1995).